Univerzita Karlova v Praze
Přírodovědecká fakulta
Katedra fyzikální a makromolekulární chemie

Diplomová práce

Ab initio kvantově chemická studie fenylacetylenových komplexů

Róbert Sedlák

2009

Školitel: prof. Ing. Pavel Hobza, DrSc.

Akademie věd, Česká republika
Ústav organické chemie a biochemie
Centrum biomolekul a komplexních molekulových systémů

Charles University in Prague
Faculty of Science
Department of Physical and Macromolecular Chemistry

Diploma thesis

Ab initio quantum chemical investigation of phenylacetylene complexes

Róbert Sedlák

2009

Advisor: prof. Ing. Pavel Hobza, DrSc.

Academy of Sciences of the Czech Republic
Institute of Organic Chemistry and Biochemistry
Center for Biomolecules and Complex Molecular Systems

I hereby declare that this thesis contains solely my original work, and has not received any outside assistance. The usage of any external data is acknowledged by cited references.

Prague, 29.04.2009 Róbert Sedlák

Acknowledgement

First, I would like to thank Professor Pavel Hobza for his kind guidance and support. I am also indebted to G. Naresh Patwari for his help and leading me. Finally, I would like to thank all members of prof. Hobza's group for their support and friendly atmosphere. I am especially grateful to Karel Berka, Martin Kabeláč, Jan Řezáč and Michal Kolář.

Contents

List of Tables **7**

List of Figures **8**

List of Abbreviations **9**

Preface **10**

1 Introduction **11**

2 Background **15**

3 Methodology and calculations **18**

3.1 Methodology 18

3.2 Calculations 20

3.2.1 Single Point calculations 20

3.2.2 Symmetry Adapted Perturbation Theory 21

4 Results and discussions **23**

4.1 Complexes of phenylacetylene with water, methanol, ammonia and methylamine 23

4.1.1 Comparison of various methods 23

4.1.2 DFT-SAPT vs. CCSD(T) results 24
4.1.3 Entropy influence 27
4.1.4 Structure probability and kinetic trapping 28
4.2 Complexes of phenylacetylene with borane-trimethylamine 30
4.2.1 Comparison of various methods 30
4.2.2 DFT-SAPT decompositions 33

5 Conclusions **35**

Bibliography **37**

Appendices **41**

List of Tables

4.1 ZPE and BSSE corrected stabilisation energies (kJ/mol) of various PHA complexes calculated using aug−cc−pVDZ basis set and ΔG for the formation of various complexes at 10 K. . . . 24

4.2 DFT−SAPT interaction energy decomposition (kJ/mol) for various complexes of PHA calculated using aug−cc−pVDZ basis set. 25

4.3 ZPE and BSSE corrected stabilisation energies (kJ/mol) for the PHA−BTMA complexes calculated at various levels of theory. 32

4.4 DFT−SAPT interaction energy decomposition (kJ/mol) for the PHA−BTMA complexes calculated using aug−cc−pVDZ basis set. 34

List of Figures

1.1 **π-electron densities of phenylacetylene** 11

1.2 **phenylacetylene-water complex** 12

1.3 **phenylacetylene-methanol complex** 13

1.4 **phenylacetylene-ammonia complex** 13

1.5 **phenylacetylene-methylamine complex** 14

2.1 **FDIR spectrum of (A) PHA, (B) PHA-Ar, (C) PHA-water, (D) PHA-methanol, (E) PHA-ammonia and (F) PHA-methylamine, in the acetylene C-H stretching region.** 16

4.1 **ΔG of PW complexes at various temperatures** 27

4.2 **ΔG of PM complexes at various temperatures** 28

4.3 **ΔG of PA complexes at various temperatures** 29

4.4 **ΔG of PMA complexes at various temperatures** 29

4.5 **phenylacetylene-borane-trimethylamineS1 complex** . . 31

4.6 **phenylacetylene-borane-trimethylamineS2 complex** . . 31

4.7 **ΔG of PBTMA complexes at various temperatures** . . 33

List of Abbreviations

6-31+G(d)	Pople‘s basis set of double zeta quality with diffuse and polarized function on heavy atoms
aug-cc-pVDZ	Dunning‘s basis set of Double Zeta quality diffuse functions
A	Ammonia
BSSE	Basis Set Superposition Error
BTMA	Borane-TriMethylAmine
CBS	Complete Basis Set
CCSD(T)	Coupled Cluster method with Single and Double excitations with taking Triple from perturbation theory
CPC	Counterpoise Correction
DFT	Density Functional Theory
DFT-SAPT	SAPT in which intramolecular correlation is treated fully by DFT
HOMO	Highest Occupied Molecular Orbital
HF	Hartree-Fock method
IP	Ionization Potential
LUMO	Lowest Unoccupied Molecular Orbital
M	Methanol
MA	Methylamine
MP2	Møller-Plesset method concerning second order correction
PBE0	Perdew-Burke-Ernzerhof hybrid type functional
PES	Potential Energy Surface
PHA	Phenylacetylene
SAPT	Symmetry Adapted Perturbation Theory
SP	Single Point calculation
TZVP	Triple Zeta Valence Polarized basis set
W	Water
ZPE	Zero Point Energy

Preface

This study is mainly focused on the theoretical investigation of the hydrogen-bonded complexes of phenylacetylene with various solvent molecules.
The work is based on experimental data of Patwari *et al.*[1–3] For this reason, a part of this thesis is focused on explanation of the foundations of the experimental study, such as spectroscopy. My intention was to introduce the reader to the basic ideas, which were followed in the Patwari‘s experimental study.

My principal goal was to make a connection between experimental and theoretical results. This includes employing theoretical tools in addressing the given questions, which often emerge from experimental work, which would eventually lead to better understanding of the observed phenomena.

Chapter 1

Introduction

Phenylacetylene (PHA) belongs to the group of molecules, which are particularly useful for model studies of non-covalent interactions. The PHA molecule is small enough for such studies, yet simultaneously it contains acetylene C–H group, two π-electron densities located on benzene ring, and acetylene C≡C triple bond Figure (1.1), which are crucial for the study of non-covalent interactions. Two latter moieties can act as hydrogen bond acceptors during a formation of hydrogen bonds, while the acidic hydrogen atom of the C–H group in acetylene moiety can act as a hydrogen bond donor. These properties make phenylacetylene an excellent choice for studies of competitive hydrogen bonding.

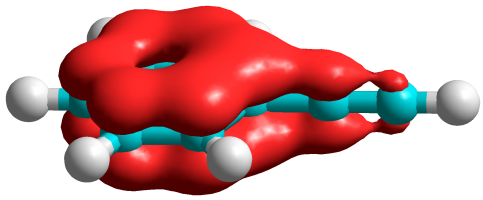

Figure 1.1: **π-electron densities of phenylacetylene**

One of the major challenges that need to be addressed in hydrogen bonding is to apriori know, how the individual functional groups in multifunctional molecules will behave upon the interactions with suitable hydrogen bonding

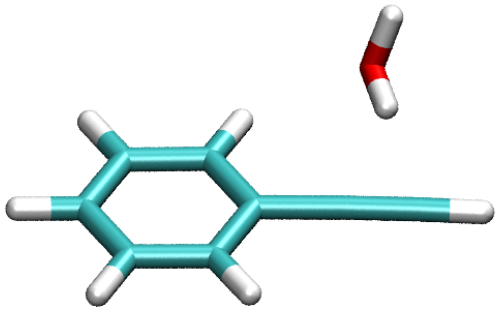

Figure 1.2: **phenylacetylene-water complex**

partners. In complex molecules the existing hydrogen-bonding pattern is the result of a competition between various possible scenarios.[4]

The experimental study of hydrogen-bonded complexes of PHA with several molecules was already made by Patwari and coworkers.[1–3] Patwari investigated complexes of PHA with different solvent molecules: water, methanol, ammonia, methylamine, borane-trimethylamine and several other alcohols and amines. Patwari *et al.* have shown that phenylacetylene domain binds with reaction partners using several different structural motifs, which are provided through several different interactions.[1–3]

For instance, PHA forms a quasi-planar cyclic complex with water incorporating O–H $\cdots$ π and C–H $\cdots$ O hydrogen bonds[1,2] Figure (1.2). In this case, one of the O–H groups of a water molecule interacts with the π-electron density of the C$\equiv$C bond, while the C–H group of the benzene ring in the ortho position forms a hydrogen bond with the oxygen atom of a water molecule. Thus, the structure of the phenylacetylene-water complex is different from both the benzene-water and the acetylene-water complexes,[5–11] even though the PHA molecule contains the moieties of both benzene and acetylene.

Moreover, the phenylacetylene-methanol complex is characterised by the presence of a single O–H$\cdots\pi$ hydrogen bond, wherein the O–H group of methanol interacts with the π-electron density of the benzene ring, similar to benzene-methanol complex[2] Figure (1.3).

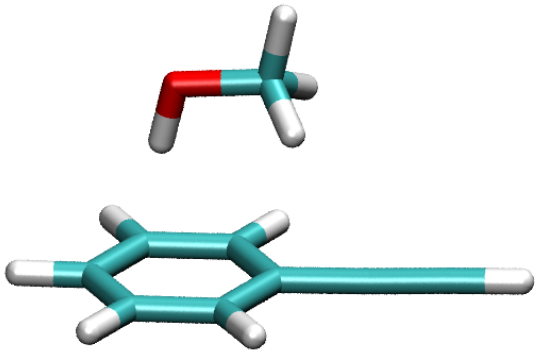

Figure 1.3: **phenylacetylene-methanol complex**

PHA forms a linear C–H $\cdots$ N "σ" hydrogen-bonded complex with ammonia[3] Figure (1.4), which is similar to acetylene-ammonia complex.[12] Phenylacetylene-methylamine complex is characterised by the presence of N–H $\cdots$ π hydrogen bond. In this complex the N–H group of methylamine interacts with the π electron density of the benzene ring[3] Figure (1.5).

Figure 1.4: **phenylacetylene-ammonia complex**

These data indicate that the methylation of an interacting partner is likely to cause a dramatic change in the structure of the moiety under investigation. Such structural change can be named "hydrogen bond switching".[4] One of the main goals of the present study is to address the question concerning the nature of the structural changes of the moiety, which can be induced by very minor (e.g. methylation) structural changes of the interacting partner.

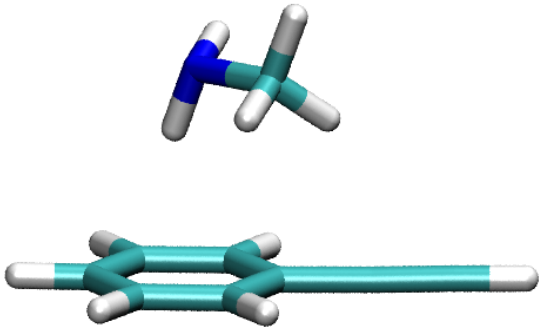

Figure 1.5: **phenylacetylene-methylamine complex**

Another aim of this study is to address the importance and nature of C–H $\cdots$ π interactions, which were investigated for the complexes of phenylacetylene with borane-trimethylamine. Such interactions are very commonly occurring in model systems Figure (1.3), as well as among the biomolecules. It should be emphasised that our understanding of the mechanisms governing the C–H $\cdots$ π interactions is far from being complete. For example, the monodentate structure of benzene-methane cluster is stabilised *via* weak electrostatic interaction.[13,14] On the other hand in the case of polycyclic aromatic ring the stability of the cluster and the orientation of the methane molecule is governed mainly by the dispersion forces.[13,14] The gas phase structure of benzene dimer is a consequence of C–H $\cdots$ π hydrogen bonding.[15] Also, Vondrasek *et al.* have shown that the stabilisation energy inside the hydrophobic core of a small protein has substantial contribution of C–H $\cdots$ π interactions involving side chains of aromatic residues.[16] Brandl *et al.* have also shown that half of all aromatic rings in proteins act as hydrogen bond acceptors.[17] Taken together, these data highlight the importance of C–H$\cdots\pi$ interaction, hence proper understanding of its nature seems to be of a crucial importance.[18]

Chapter 2

Background

The main experimental tools used by Patwari and his coworkers to study the phenylacetylene (PHA) and its complexes were IR and UV spectroscopy. The details of the experimental setup are presented in Ref. 2 and references therein. The IR spectra of PHA and PHA complexes with water, argon, methanol, ammonia and methylamine in C–H stretching region were recorded using IR-UV double resonance spectroscopic method using either fluorescence or ion detection technique.[4] These spectra are showed in Figure 2.1. From these spectra a valuable information about the perturbation of the structure of acetylene group, the solvent-solute interactions, which are mediated by either acetylene moiety or the benzene ring, can be gathered.

The IR spectrum of isolated PHA Figure 2.1 A contains two relatively symmetric transitions at 3325 cm^{-1} and 3343 cm^{-1}. These can be interpreted as the consequence of Fermi resonance coupling between the acetylene C-H stretching vibration and a combination bend. This combination bend consists of one quantum of C≡C stretching and two quanta of C≡C–H out-of-plane bend.[19] Upon the interactions between a solvent molecule and C≡C–H group through the C≡C π-electron density or the C–H bond, the transitions at 3325 cm^{-1} and 3343 cm^{-1} disappear.[20] The IR spectrum of the PW complex (Figure 2.1) clearly shows that the water molecule interacts with C≡C bond.[1] There are no transitions at 3325 cm^{-1} and 3343 cm^{-1}. In the case of PM, the structure of acetylene group remains unperturbed.

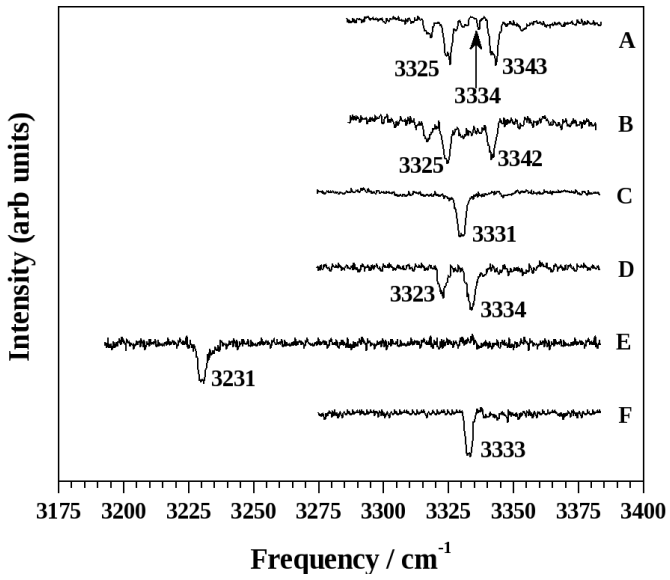

Figure 2.1: **FDIR spectrum of (A) PHA, (B) PHA-Ar, (C) PHA-water, (D) PHA-methanol, (E) PHA-ammonia and (F) PHA-methylamine, in the acetylene C-H stretching region.**

The shift of the O–H bond for methanol molecule clearly shows that the O–H bond interacts with π-electron density of the benzene ring[2], in a similar fashion than in the benzene-methanol complex.[2] For the PA complex the assignment of the structure is much more straightforward. The quasi-linear C–H$\cdots$N hydrogen bond is formed.[3] The evidence of this formation emerges from the fact is that C–H stretching region is shifted towards lower frequencies by 103 cm^{-1}.[3] The PMA spectrum shows that acetylene group does not interact with methylamine. Moreover, the C–H stretching vibration remains almost the same, compared to the isolated PHA, which indicates no formation of the C–H$\cdots$N hydrogen bond.[3]

This is quite surprising, since the addition of the methyl group to the solvent molecule increases its basicity. This should cause a formation of the C–H$\cdots$N hydrogen bond.[4] It should be emphasised here, that the solvent was chosen rationally, in order to include the series of compounds with proton affinity increasing: water, methanol, ammonia and methylamine. The analysis of the geometries of the PMA complexes lead to the conclusion

that the N–H$\cdots\pi$(benzene) interaction together with methyl C–H$\cdots$C$\equiv$C bond interaction were present.[3]

Another striking feature of PMA complexes is related to their unusual hydrogen–bonding properties. It is known that the alkyl amines usually act as excellent hydrogen bond acceptors. Surprisingly, methylamine acted as a hydrogen bond donor.[4] Very interesting feature of the PHA complexes is vast difference between the intermolecular structure of water and methanol complexes, and similarity between the ammonia and methylamine complexes. These observations can be summarised as methyl group–induced hydrogen-bond switching. To understand these phenomena, high level *ab initio* quantum chemical calculations were carried out.[4]

Chapter 3

Methodology and calculations

3.1 Methodology

As already mentioned in the "Background" section, it is clear that there is only one experimentally observed structure for each solvent molecule. This implies that for each type of complex there is a unique structural motif, which is predominantly formed and may be experimentally observed. However, one should bear in mind that phenylacetylene (PHA) molecule contains several binding moieties, which has been mentioned in the Introduction.

All complexes under investigation are non-covalent, which is characterised by the presence of very weak interactions. Hence, the high-accuracy quantum chemistry methods, covering the electron correlation, were required for this study (e.g. Møller-Plesset second order perturbation method (MP2)[21] and Coupled Cluster method covering single, double and triple electron excitations (CCSD(T)).[22,23] Hartree-Fock (HF) method does not include electron correlation and therefore could not been used.[24] Both MP2 and CCSD(T), however, do not provide any information about the character of the interaction studied. Thus, the Symmetry Adapted Perturbation Theory[25] combined with Density Functional Theory[26,27] (DFT-SAPT) calculations were additionally performed.[28]

The first task was to find local minima on potential energy surface (PES),

for each of the complexes studied: PHA with water (W), ammonia (A), methanol (M) and methylamine (MA). It has been done using MP2 gradient optimisation at aug-cc-pVDZ level. It was reported that such accuracy should be appropriate for this kind of complexes.[29]

Initial structures corresponding to the local minima were based on Patwari's data. The structures were optimised as described above. For the PHA-BTMA complex the experimental structural data were missing, hence the guessed structure was used. Such guess was based on the experimental data for structural motifs, present in other complexes. In the case of PHA-BTMA complex, the preliminary optimisations were done at MP2/6-31+G(d) level.[30]

For each solvent molecule (W, M, A, MA) three structural motifs: S1, S2 and S3 were considered. For BTMA just S1 and S2 structures were taken into account.

1. The S1 structure can be characterised by the presence of quasi-linear C–H$\cdots$X (O, N) hydrogen bond (Figure 1.4).

2. In the S2 structure the specific X (O, N)–H$\cdots\pi$(benzene ring) interaction is found (Figure 1.3 and 1.5).

3. The S3 structure is the quasi-cyclic complex. This complex has two features: (N, O) X–H$\cdots\pi$(C$\equiv$C) interaction and (O, N) X$\cdots$C–H (acetylene) hydrogen bond (Figure 1.2).

For a clarity, the following labels were assigned to each structure. The first 2-3 letters in the label were abbreviation of the names of the cluster compounds, and last two characters specified which PHA binding side interacted with the solvent molecule. Example: PMS2 = phenylacetylene-methanol complex, where O–H$\cdots\pi$(benzene) hydrogen bond is present. PWS3 =

phenylacetylene-water (PW) complex with the quasi cyclic S3 geometry. Such labelling systems is consistently used throughout the thesis. All optimisations were followed by frequency calculation, to assure that investigated structures corresponded indeed to the local minima (no negative/imaginary frequencies should be present for the optimized structure).

3.2 Calculations

3.2.1 Single Point calculations

Single point (SP) calculations at different level of theory were then performed on the most stable geometries. The SP calculations were carried at either CCSD(T) or MP2 level of theory in combination with aug-cc-pVDZ basis set[31] calculations for interaction energies for all theoretically predicted complexes. The density fitting was used consistently.[32,33] It is generally known that MP2 method overestimates the stabilisation energy (Ref 34), hence the CCSD(T) single point calculations with aug-cc-pVDZ basis set were employed, in order to provide more accurate results.

All interaction energies were corrected for basis set superposition error (BSSE) with use of counterpoise correction (CPC)[34] and for zero point energy (ZPE). Including the ZPE we pass from interaction energy to interaction enthalpy at 0 K.

Since experiments were realized at non-zero temperatures the entropy should be included as well. The thermodynamic characteristics (entropy, Gibbs energy, enthalpy) were calculated using rigid rotor-harmonic oscillator-ideal gas approximations.

Since the temperature of experiment is not known we calculated the Gibbs energy at various temperatures, from 10 to 300 K with step of 10 K.

The change of Gibbs energy was evaluated at MP2/aug-cc-pVDZ level. The interaction energy part was replaced by more accurate interaction energy determined at the CCSD(T)/aug-cc-pVDZ level (BSSE correction was included). The deformation energy was expected to be small and was not considered.

In the case of PHA-BTMA complex the CCSD(T)/CBS interaction energies were calculated. These energies were determined as a sum of MP2/CBS energies and CCSD(T) correction term Eqn. (3.1).

$$\Delta E^{CBS}_{CCSD(T)} = \Delta E^{CBS}_{MP2} + \left(\Delta E_{CCSD(T)} - \Delta E_{MP2}\right)_{mediumbasisset} \tag{3.1}$$

The method takes advantage of the fact that both the CCSD(T) and MP2 methods exhibit approximately the same basis set dependence.[35] MP2 correlation energies have been extrapolated using aug-cc-pVDZ and aug-cc-pVTZ basis sets. We used Kim and coworkers extrapolation.[36] The Kim extrapolation assumes that curves of interaction energies corrected as well as uncorrected for the basis set superposition meet each other in the CBS limit. The CCSD(T) correction term was determined at the aug-cc-pVDZ basis set level.

3.2.2 Symmetry Adapted Perturbation Theory

Symmetry adapted perturbation theory[25] using density functional theory[26,27] (DFT-SAPT)[28] calculations were carried out for all complexes of PHA and also for nucleic acid base pair taken from DNA crystal geometry. The study of nucleic acid base pair is attached in appendix.

The interaction energy is given by as a sum of various energies (Eqn. 3.2):

$$E^{DFT-SAPT}_{int} = E^{(1)}_{Pol} + E^{(1)}_{Ex} + E^{(2)}_{Ind} + E^{(2)}_{Ex-Ind} + E^{(2)}_{Disp} + E^{(2)}_{Ex-Disp} + \delta HF \tag{3.2}$$

where:

$E^{(1)}_{Pol}$ is electrostatic term,

$E_{Ex}^{(1)}$, $E_{Ex-Ind}^{(2)}$, $E_{Ex-Disp}^{(2)}$ are exchange-repulsion terms,

$E_{Ind}^{(2)}$ is induction term,

$E_{Disp}^{(2)}$ is dispersion term,

δHF is Hartree-Fock correction term,

DFT-SAPT decomposition was calculated with aug-cc-pVDZ basis set in combination with PBE0AC exchange-correlation functional with density fitting approximation.[37] The PBE0AC functional in combination with aug-cc-pVDZ basis set was shown to give accurate first-order terms as well as induction and exchange terms,[37] while dispersion contribution is underestimated approximately by 10-20 %.[38] We implemented gradient-controlled shift procedure which needs a difference shift between the vertical ionisation potential (IP) and the highest occupied molecular orbital (HOMO) energy of the DFT method used as an input.[37] The IPs were calculated at the PBE0/TZVP level, while the HOMO values were taken from the calculation with aug-cc-pVDZ basis set.

All calculations were carried out with Gaussian 03[20] and Molpro 06[39] packages. The CCSD(T) calculations for the CCSD(T) correction term were performed at the CHINOOK supercomputer (USA)[40].

Chapter 4

Results and discussions

4.1 Complexes of phenylacetylene with water, methanol, ammonia and methylamine

4.1.1 Comparison of various methods

The experimental results based on the spectroscopic measurements (see Background section) indicated the formation of PWS3, PMS2, PAS1, and PMAS2 structures. These experimental results have been supplemented by MP2/aug-cc-pVDZ stabilisation energies corrected for ZPE and BSSE,[1–3] performed on geometries optimised at MP2/aug-cc-pVDZ level.

In Table (4.1) stabilisation energies corrected for BSSE and ZPE are showed. For methanol (PMS2) and ammonia (PAS1) complexes we have found that the experimentally observed structures are the most stable ones. Contrary, in the case of water (PWS3) and methylamine (PMAS2) complexes, the experimental structures corresponded to the higher energy minima.[4]

The CCSD(T) stabilisation energies corrected for ZPE, taken from MP2/aug-cc-pVDZ calculation, are also showed in Table 4.1. For CCSD(T) approach, the experimentally observed PWS3, PMS2, and PAS1 structures represented respective global minima. However, PMAS2 experimental structure was represented only by a local minimum with higher energy.[4]

Structure	E^{MP2}	$E^{CCSD(T)}$	ΔG_{10K}
PWS1	-6.4	-6.2	-5.6
PWS2	-8.1	-6.5	-6.2
PWS3	-7.6	-7.1	-6.7
PMS1	-9.8	-9.1	-8.2
PMS2	-13.6	-9.6	-8.5
PMS3	-13.1	-9.5	-7.8
PAS1	-8.7	-8.2	-7.2
PAS2	-5.4	-3.2	-2.7
PAS3	-6.7	-5.9	-5.4
PMAS1	-12.4	-11.3	-9.9
PMAS2	-10.6	-6.4	-5.4
PMAS3	-12.1	-9.4	-8.4

Table 4.1: ZPE and BSSE corrected stabilisation energies (kJ/mol) of various PHA complexes calculated using aug−cc−pVDZ basis set and ΔG for the formation of various complexes at 10 K.

The differences in the stabilisation energies of all three isomers were quite marginal in the case of water and methanol 0.9 kJ/mol and 0.5 kJ/mol, respectively. The picture was quite different for ammonia and methylamine complexes. In case of A complexes, the energy difference between two most stable structures was 2.3 kJ/mol. However, for MA complexes the experimentally observed PMAS2 structure was less stable by 4.9 kJ/mol than the global minimum (PMAS1).[4]

4.1.2 DFT-SAPT vs. CCSD(T) results

The DFT-SAPT decomposition of interaction energy was done with aug-cc-pVDZ basis set for all twelve complexes. Results are showed in Table 4.2. The last column in the table represents DFT-SAPT stabilisation energies corrected for ZPE, taken from MP2/aug-cc-pVDZ calculations.

Structure	$E_{el}^{(1)}$	$E_{I}^{(2)}$	$E_{D}^{(2)}$	$E_{Ex}^{(1)}$	δHF	E^{SAPT}	$E^{SAPT}{}_{ZPE}$
PWS1	-17.0	-2.6	-6.4	17.4	-2.0	-10.6	-6.3
PWS2	-11.9	-2.7	-13.1	18.2	-1.5	-11.0	-7.3
PWS3	-25.5	-4.8	-13.6	32.2	-3.5	-15.2	-9.0
PMS1	-20.9	-3.1	-10.2	24.8	-2.8	-12.2	-9.0
PMS2	-17.4	-3.2	-26.1	36.2	-3.0	-13.5	-10.2
PMS3	-20.2	-3.2	-25.6	37.7	-3.2	-14.6	-10.7
PAS1	-24.9	-4.1	-8.4	27.0	-3.8	-14.2	-8.8
PAS2	-9.3	-1.4	-14.4	19.1	-1.4	-7.4	-3.9
PAS3	-22.4	-3.5	-13.8	29.8	-2.9	-12.8	-7.8
PMAS1	-29.2	-4.7	-12.7	35.9	-5.2	-16.0	-11.8
PMAS2	-15.4	-1.5	-26.3	35.2	-2.6	-10.6	-7.1
PMAS3	-25.5	-3.3	-23.1	41.1	-3.6	-14.4	-10.8

Table 4.2: DFT−SAPT interaction energy decomposition (kJ/mol) for various complexes of PHA calculated using aug−cc−pVDZ basis set.

In the case of experimentally observed PWS3 structure, electrostatics along with dispersion interactions were the most important interactions in terms of stabilising the complex (Table 4.2). The induction and δHF terms were marginal. For the PWS1 structure with the 'classic' hydrogen bond, the electrostatics was clearly the main stabilising factor, followed by the dispersion and the induction term. Stabilising contribution emerging from δHF term was again the smallest one. PWS2 isomer had a very different energy decomposition in comparison with PWS1 isomer. Therein, mainly dispersion was responsible for the attraction between the cluster compounds. Electrostatics was almost as strong as dispersion interaction, however. Yet again induction and δHF contributions were the smallest ones. The energy differences between the local minima structures of water complexes were in the case of DFT-SAPT calculations larger than obtained by CCSD(T). It is worth to mention that the order of the complex stability remained the same.

The energy decomposition for PMS2 structure clearly indicated that the dis-

persion interaction assisted by electrostatics are the main contributors to the stabilisation of the complex. Energetically the most stable PMS3 isomer had the largest stabilisation contribution coming from dispersion, -25.6 kJ/mol, -20.2 kJ/mol came from the electrostatic term, and -3.2 kJ/mol originated from the induction and δHF. Less stable S1 structure was stabilised mainly by the electrostatic interaction, which was a typical feature for all four S1 isomers.

In the case of methanol complexes the order in stability of the minima calculated with DFT-SAPT changed compares to the CCSD(T) results. The energy gap between the most stable structure and the rest increased from 0.5 kJ/mol for CCSD(T) approach to 1.7 kJ/mol for DFT-SAPT calculations.

The electrostatics was the dominant attractive interaction also in the case of experimentally observed PAS1 structure. The second biggest attractive interaction was the dispersion one. This was twice as attractive as the induction and δHF terms, which were comparable with each other. The PAS3 isomer had similar energy decomposition pattern to already mentioned PAS1. The big difference between PAS3 and PAS1 isomers was due to the importance of the dispersion contribution in the PAS3 structure. The PAS2 isomer was the only structure, where the largest attractive contribution was a dispersive one.

Experimentally observed PMAS2 isomer was once again the only structure from MA complexes where the dispersion played the major stabilising role. This trend was observable for all S2 complexes with different solvent molecules. The most stable PMAS1 isomer had its electrostatic term more than twice as large as a dispersive one. In the case of the PMAS3 structure both electrostatic and dispersive terms were almost equally large.

For A and MA complexes, both theoretical approaches provided the same order in the stability of local minima structures. Also, the energy difference between the most and the least stable structures were almost the same.

For all twelve complexes, there was a strong correlation between the E_{ind} and δHF term, which is in agreement with already published data.[41]

4.1.3 Entropy influence

Considering the fact that the temperature during the cluster formation is not equal zero but its value is not known, there is a need to include the influence of entropy into the calculations. Therefore we have calculated Gibbs energy for complex formation for various temperatures ranging from 10 to 300 K in steps of 10 K. The results (in the form of plots) are presented in Figures 4.1, 4.2, 4.3, 4.4 and 4.7. The ΔG values at 10 K are showed in Table 4.1. The plots suggest that the complexes are probably formed below 100 K. This is in agreement with the fact that experimental temperature in the case of PHA expansion to vacuum is approximately 4 K.[42]

The Gibbs energy of cluster formation reached negative values somewhere below 80 K for W complexes Figure 4.1. Below this temperature the PWS3 structure was the most stable one, what is supported by experimental results[1]. See also column ΔG in Table 4.1.

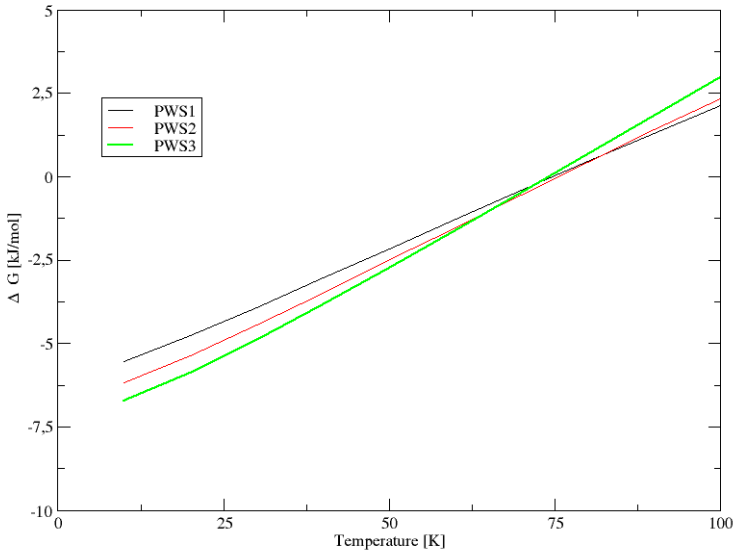

Figure 4.1: **ΔG of PW complexes at various temperatures**

In the case of M complexes (Figure 4.2) the S2 structure at 10 K was more stable than S1 and S3 structures by -0.3 kJ/mol and -0.7 kJ/mol, respec-

tively. The S1 and S3 are almost isoenergetic. Based on this difference, the population of S1 and S3 structures should be about 2 % compare to S2. [4]

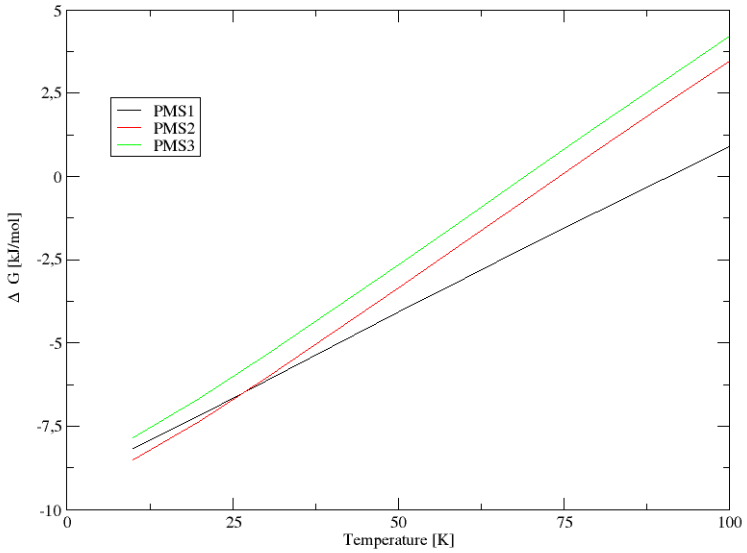

Figure 4.2: **ΔG of PM complexes at various temperatures**

Experimentally observed PAS1 isomer was the most preferred over a full range of temperatures (Figure 4.3) and at 10 K, it was more stable than PAS3 and PAS2 isomers by 1.8 kJ/mol and 4.5 kJ/mol, respectively.

However the populations of PHA complexes with MA were in disagreement with experimental results. Experimentally observed PMAS2 was less preferred in the whole range of temperatures (Figure 4.4). At the lowest temperature 10 K, the PMAS2 isomer was less stable by 3.0 kJ/mol and 4.5 kJ/mol, respectively, as compared to the PMAS3 and PMAS1 isomers.

4.1.4 Structure probability and kinetic trapping

It is clear that there must be other factors playing important role in these interactions. In particular, for M and MA complexes which were not covered by calculations. The disagreement between the theoretical and experimental data for M and MA complexes could be explained as follows:

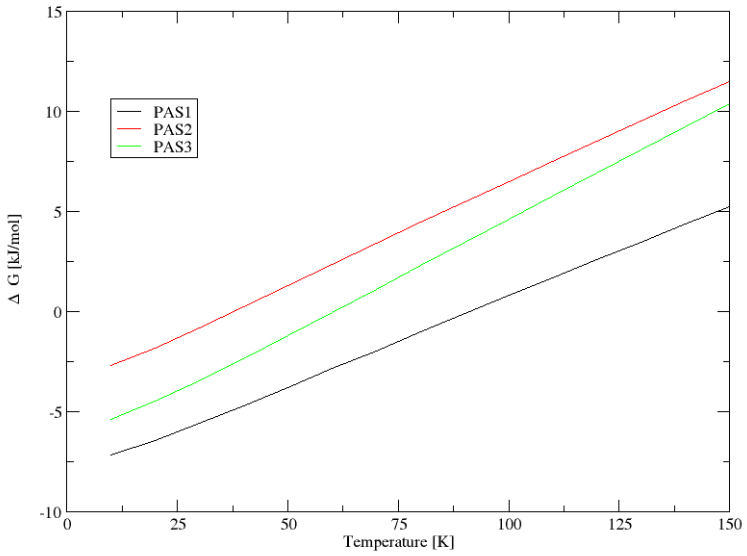

Figure 4.3: **ΔG of PA complexes at various temperatures**

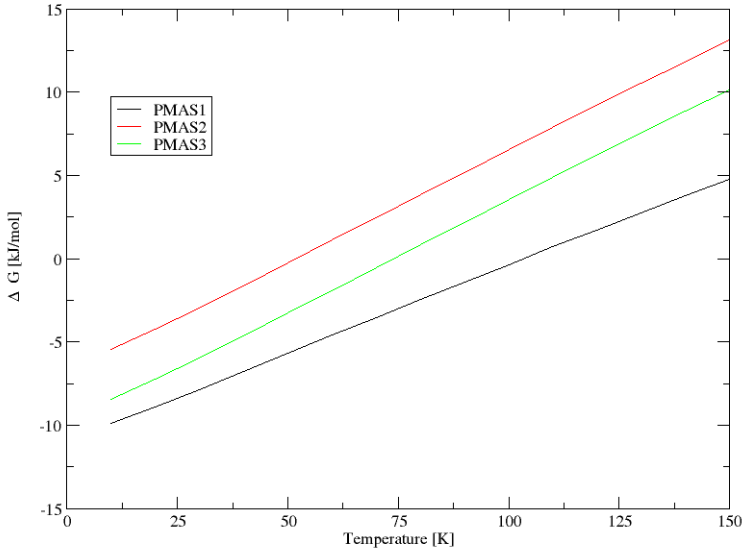

Figure 4.4: **ΔG of PMA complexes at various temperatures**

When the clusters are formed at the low temperature *via* a collision between the PHA and a solvent molecule, there is more likely that the S2

isomer will be formed, rather than the S1 or S3 isomers. This hypothesis is based on the fact that the benzene ring provides a bigger cross-section area for the interaction compared to the remaining two binding sites (C≡C bond and hydrogen bond).[4] This feature cannot be covered be the method of ΔG used, due to the approximations beneath (i.e. ideal gas-rigid rotor-harmonic oscillator). This probability aspect along with already mentioned small (0.4 kJ/mol) energy preference of PMS2 isomer are the most important factors which are responsible for the unique formation of the PMS2 structure.[4]

In the case of MA complexes, an exclusive formation of the S2 structure, which is not supported by stabilisation energy and ΔG calculations, is suggested to emerge from the cross-section entropy effect and the kinetic trapping.

The kinetic trapping may be described as follows: Upon the S2 structure formation (as the most probable isomer based on cross-section entropy), at the low experimental temperature, the probability of crossing the barrier between S2 structure and another one, is low. This idea is based on the concept that S2 local minimum structure is surrounded with high energy barriers on a given potential energy surface (PES).[4] It should be mentioned that this explanation is not supported by any kind of calculations and at this point has a status of a hypothesis.

4.2 Complexes of phenylacetylene with borane-trimethylamine

4.2.1 Comparison of various methods

The experimental results for PBTMA complexes clearly showed that there was only one experimentally-observed structure. Analyses of the spectra and comparison with other hydrogen bonded complexes lead Patwari *et al.* to the conclusion that BTMA interacted primarily with the π-electron density

of the benzene ring.[18] The PBTMAS2 isomer was formed. The structures of local minima of PBTMA complexes are illustrated in the Figures 4.5 and 4.6

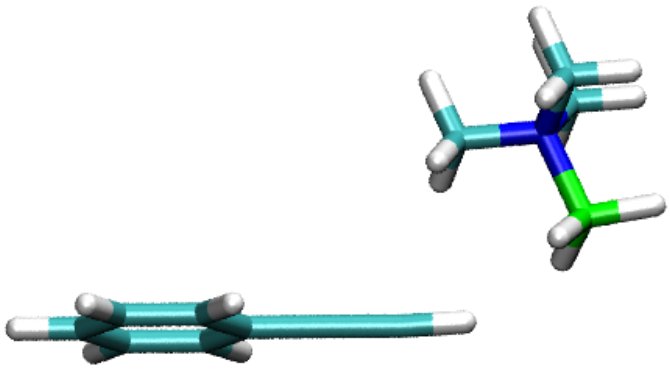

Figure 4.5: **phenylacetylene-borane-trimethylamineS1 complex**

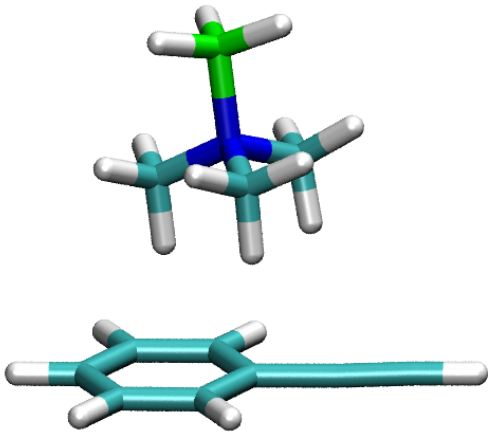

Figure 4.6: **phenylacetylene-borane-trimethylamineS2 complex**

For PHA complexes, the same calculations were performed with borane-trimethylamine (BTMA) as with W, M, A, and MA. Further, the CCSD(T)/ CBS calculations were carried out.

The optimal geometries of local minima structures were found using MP2/aug-cc-pVDZ level of theory. The stabilisation energies for given geometries, at different levels of theory, same as before, were performed. Namely, CCSD(T)/aug-cc-pVDZ, MP2/aug-cc-pVDZ also DFT-SAPT/aug-cc-pVDZ, and CCSD(T)/CBS. In accordance with the methodology applied previously, all stabilisation energies have been corrected for BSSE and ZPE (Table 4.3).

Structure	$E^{MP2}_{aug-cc-pVDZ}$	$E^{CCSD(T)}_{aug-cc-pVDZ}$	$E^{DFT-SAPT}_{aug-cc-pVDZ}$	$E^{CCSD(T)}_{CBS}$
PBTMAS1	-12.4	-11.1	-11.5	-14.1
PBTMAS2	-16.5	-10.9	-11.7	-15.6

Table 4.3: ZPE and BSSE corrected stabilisation energies (kJ/mol) for the PHA−BTMA complexes calculated at various levels of theory.

The PBTMAS2 structure at the MP2/aug-cc-pVDZ level was more stable than the PBTMAS1 structure by 4.1 kJ/mol, what was in agreement with experimental data. We have used CCSD(T)/aug-cc-pVDZ approach for more accurate comparison of these two systems, because of well known feature of the MP2 to overestimate dispersion contribution.

The CCSD(T)/aug-cc-pVDZ data provided results where the PBTMAS1 isomer was more stable by 0.2 kJ/mol, as compared to the PBTMAS2. That contradicts the experimental results. We obtained same energy difference for S1 and S2 isomers by the DFT-SAPT decomposition. In this case was the order of statibility of the considered minima in agreement with experimental results.

The energy difference between PBTMAS1 and PBTMAS2 structures was 0.6 kJ/mol. Thus, we have carried out the most accurate calculations. Namely, the CCSD(T)/CBS with Kim extrapolation of MP2 energy were performed. [36] With this level of theory, the experimentally observed PBTMAS2 isomer was more stable than the PBTMAS1 isomer by 1.5 kJ/mol. [18]

The ΔG calculations were performed in the same way as in previous cases only with one exception. The MP2/aug-cc-pVDZ stabilisation energy was substituted by CCSD(T)/CBS stabilisation energy. The ΔG of the complex formation as a function of temperature is depicted on Figure 4.7. For both structures, ΔG reached negative values in temperatures below 110 K. The S2 structure was stable for lower temperatures, starting below 90 K.[18]

The formation of the PBTMAS2 cluster (-15.6 kJ/mol) was preferred over the formation of the PBTMAS1 cluster (-12.8 kJ/mol) at 10 K (Figure 4.7),[42] what is in accordance to the experimental data.[18]

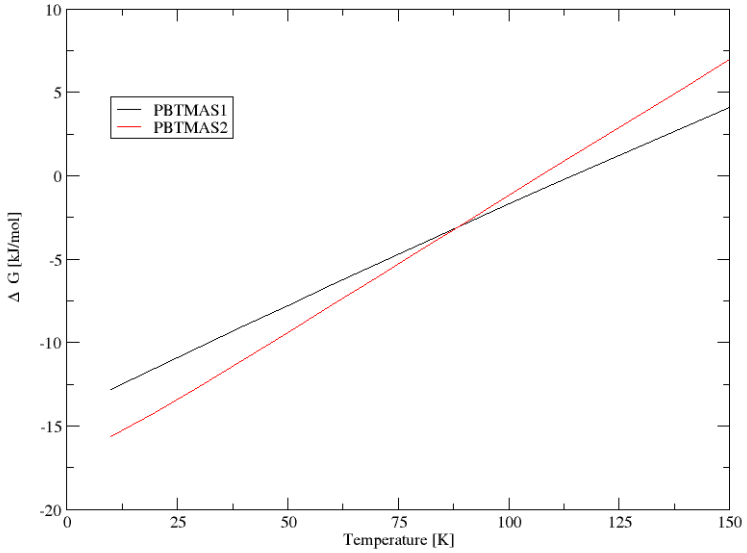

Figure 4.7: **ΔG of PBTMA complexes at various temperatures**

4.2.2 DFT-SAPT decompositions

The DFT-SAPT decomposition of stabilisation energies of PBTMA complexes is showed in Table 4.4. For the PBTMAS1 structure the electrostatic term (-20.8 kJ/mol) was more attractive than the dispersion term (-16.4 kJ/mol). The contributions from the induction and δHF terms were marginal.[18]

Structure	$E_{el}^{(1)}$	$E_{I}^{(2)}$	$E_{D}^{(2)}$	$E_{Ex}^{(1)}$	δHF	E^{SAPT}
PBTMAS1	-20.8	-2.6	-16.4	28.5	-2.7	-14.0
PBTMAS2	-21.4	-2.5	-34.3	47.3	-3.7	-14.6

Table 4.4: DFT−SAPT interaction energy decomposition (kJ/mol) for the PHA−BTMA complexes calculated using aug−cc−pVDZ basis set.

The electrostatic term for the PBTMAS2 structure (-21.4 kJ/mol) was similar to the electrostatic contribution for the PBTMAS1 structure (-20.8 kJ/mol). This finding is surprising mainly because the stacked structures (the structures stabilised *via* dispersion interaction) usually have significantly lower stabilisation energy, emerging from the electrostatics, compared to the structures with 'conventional' hydrogen bonds (structures stabilised *via* electrostatic and induction interactions).[41]

The main difference in the decomposition of the analysed minima laid within the dispersion contribution to the total stabilisation. For the S2 cluster (-34.3 kJ/mol) dispersion played much more important role compared to the S1 cluster[18] (-16.4 kJ/mol). Due to the significant exchange-repulsion term in the decomposition for the S2 cluster the total stabilisation energies for both clusters S1 and S2 were comparable (see Table 4.4). The picture remained unchanged after including the ZPE correction.[18]

The stabilisation energies obtained by the DFT-SAPT/aug-cc-pVDZ and the CCSD(T)/aug-cc-pVDZ methods were underestimated compared to the CCSD(T)/CBS data. This is in agreement with the results published by Hesselmann and Jansen.[43] The DFT-SAPT analysis strongly indicated that many of the C–H$\cdots\pi$ hydrogen-bonded PBTMA complexes were stabilised primarily through dispersion interactions with significant contribution from electrostatics and a very small induction contribution.[18]

Chapter 5

Conclusions

The phenylacetylene-water complex, which is characterised by the presence of quasi-cyclic arrangement with the O–H$\cdots$O and C–H$\cdots$O interaction, was the most stable structure. This statement was verified by the calculations of stabilisation energies and ΔG of formation for all the three conformers. The PWS3 structure was more stable by 0.6 kJ/mol and 0.9 kJ/mol than PWS2 and PWS1, respectively. The ΔG difference between PWS3 and other structures is even larger.

In the case of the phenylacetylene-methanol complex, the most stable structure was the PMS2 structure, which was by about 0.1 kJ/mol and 0.4 kJ/mol respectively more stable than the other two structures. If the ΔG values are considered, the difference between PMS2 structure and the other two structures increased further.

The stabilisation energy and ΔG calculations for complex of PHA with ammonia revealed that the PAS1 structure was the most stable structure among the PHA ammonia complexes.

The theoretical results of water, ammonia and methanol complexes were found in good agreement with the experiment. The exception was the PMAS2 structure, which experimental structure was the least stable one. This discrepancy could be caused by either kinetic trapping or entropy effect.

The present results showed that the influence and interplay between thermo-

dynamic stability and temperature contribution, entropy factors, and kinetic trapping, are very crucial during the formation of non-covalent complexes in the gas phase.

The DFT-SAPT calculation showed that electrostatic is the most important type of interaction, in the case of water and ammonia complexes, whereas dispersion played the predominant role among all methanol and methylamine interactions. The DFT-SAPT results indicated that the ratio between electrostatic and dispersion terms had determined the kind of these two interactions, which would be dominant. These results are directly linked to experimentally observed hydrogen bond switching.

According to the results obtained, the S1 and S2 structures of borane-trimethylamine and PHA complexes were nearly isoenergetic at CCSD(T)/ aug-cc-pVDZ level of theory. Improving the level of calculations to the CBS limit lead to the energy separation of these two structures, and S2 structure became more stable. The Gibbs energy calculations clearly showed that formation of the S2 complex is preferred to the S1 structure. DFT-SAPT calculations indicated that the dispersion together with electrostatic were the most important stabilisation factors for the experimentally observed S2 complex.

In the case of the water, methanol and ammonia complexes, the CCSD(T)/ aug-cc-pVDZ results agreed well with the experimental data. The energy differences between structures were quite small for the complexes of methanol. However, the complexes containing water and ammonia had substantial gaps between the considered minima. The calculated energies of methylamine complex did not agree with the experimental results, hence it is likely that the PMAS2 structure may be kinetically trapped.

DFT-SAPT analysis indicated that electrostatic contribution to the stabilisation of experimentally observed PHA complexes with water and ammonia played predominant role. The dispersion played an equally important role in methanol and methylamine complexes. In borane-trimethylamine complexes the picture was quite different. For experimentally observed complex, both electrostatic and dispersion were dominant attractive forces.

Bibliography

[1] Singh P. C.; Bandyopadhyay B.; Patwari G. N. *J. Phys. Chem. A*, 2008, 112, 3360.

[2] Singh P. C.; Patwari G. N. *J. Phys. Chem. A*, 2008, 112, 5121.

[3] Singh P. C.; Patwari G. N. *J. Phys. Chem. A*, 2008, 112, 4426.

[4] Sedlak R.; Hobza P.; Patwari G. N. *J. Phys. Chem. A*, in press.

[5] Engdahl A.; Nelander B. *J. Phys. Chem.*, 1985, 89, 2860.

[6] Wanna J.; Menapace J. A.; Bernstein E. R. *J. Chem. Phys.*, 1986, 85, 1795.

[7] III; Blake G. A. Suzuki S.; Green P. G.; Bumgarner R. E.; Dasgupta S.; Goddard W. A. *Science*, 1992, 257, 942.

[8] Pribble R. N.; Garrett A. W.; Haber K.; Zwier T. S. *J. Chem. Phys.*, 1995, 103, 531.

[9] Gutowsky H. S.; Emilsson T.; Arunan E. *J. Chem. Phys.*, 1993, 99, 4883.

[10] Engdahl A; Nelander B. *Chem. Phys. Lett.*, 1983, 100, 129.

[11] Peterson K. I.; Klemperer W. *J. Chem. Phys.*, 1984, 81, 3842.

[12] Fraser G. T.; Leopold K. R.; Klemperer W. *J. Chem. Phys.*, 1984, 80, 1423.

[13] Tsuzuki S.; Fujii A. *Phys. Chem. Chem. Phys.*, 2008, 10, 2584.

[14] Tsuzuki S.; Honda K.; Fujii A.; Uchimarua T.; Mikami M. *Phys. Chem. Chem. Phys.*, 2008, 10, 2860.

[15] Arunan E.; Gutowsky H. S. *J. Chem. Phys.*, 1993, 98, 4294.

[16] Vondrasek J.; Bendova L.; Klusak V.; Hobza P. *J. Am. Chem. Soc.*, 2005, 127, 2615.

[17] Brandl M.; Weiss M. S.; Jabs A.; Suhnel J.; Hilgenfeld R. *J. Mol. Biol.*, 2001, 307, 357.

[18] Maity S.; Sedlak R.; Hobza P.; Patwari G. N. *J. Phys. Chem. A*, submitted.

[19] Stearns J. A.; Zwier T. S. *J. Phys. Chem. A*, 2003, 107, 10717.

[20] Jr.; Vreven T.; Kudin K. N.; Burant J. C.; Millam J. M.; Iyengar S. S.; Tomasi J.; Barone V.; Mennucci B.; Cossi M.; Scalmani G.; Rega N.; Petersson G. A.; Nakatsuji H.; Hada M.; Ehara M.; Toyota K.; Fukuda R.; Hasegawa J.; Ishida M.; Nakajima T.; Honda Y.; Kitao O.; Nakai H.; Klene M.; Li X.; Knox J. E.; Hratchian H. P.; Cross J. B.; Bakken V.; Adamo C.; Jaramillo J.; Gomperts R.; Stratmann R. E.; Yazyev O.; Austin A. J.; Cammi R.; Pomelli C.; Ochterski J. W.; Ayala P. Y.; Morokuma K.; Voth G. A.; Salvador P.; Dannenberg J. J.; Zakrzewski V. G.; Dapprich S.; Daniels A. D.; Strain M. C.; Farkas O.; Malick D. K.; Rabuck A. D.; Raghavachari K.; Foresman J. B.; Ortiz J. V.; Cui Q.; Baboul A. G.; Clifford S.; Cioslowski J.; Stefanov B. B.; Liu G.; Liashenko A.; Piskorz P.; Komaromi I.; Martin R. L.; Fox D. J.; Keith T.; Al-Laham M. A.; Peng C. Y.; Nanayakkara A.; Challacombe M.; Gill P. M. W.; Johnson B.; Chen W.; Wong M. W.; Gonzalez C.; Pople J. A. Frisch M. J.; Trucks G. W.; Schlegel H. B.; Scuseria G. E.; Robb M. A.; Cheeseman J. R.; Montgomery J. A. *Gaussian 03, Revision A.1; Gaussian, Inc.: Wallingford, CT*, 2003.

[21] Moller Ch.; Plesset M. S. *Phys. Rev.*, 1934, 46, 618.

[22] Kucharski S. A. Noga J. Bartlett R. J., Watts J. D. *Chem. Phys. Lett.*, 1990, 165, 513.

[23] Cizek J. *J. Chem. Phys.*, 1966, 45, 4526.

[24] Hartree D. R.; Fock V. A. *Hartree-Fock Self-Consistent Field method*, 1927,1930.

[25] Jerziorski B.; Szalewicz K.; Mosyznski R. *Chem. Rev.*, 1994, 94, 1886.

[26] Kohn W. Hohenberg P. *Phys. Rev.*, 1964, 136, B864.

[27] Sham L. J. Kohn W. *Phys. Rev. Soc.*, 1965, 140, A1133.

[28] Fraser G. T.; Leopold K. R.; Klemperer W. *J. Chem. Phys.*, 1984, 80, 1423.

[29] Dabkowska I.; Jurecka P.; Hobza P. *J. Chem. Phys.*, 2005, 122, 204322.

[30] Ditchfield R.; Hehre W. J.;Pople J. A. *J. Chem. Phys.*, 1971, 54, 724.

[31] Dunning T. H. Jr. *J. Chem. Phys.*, 1989, 90, 1007.

[32] Feyereisen M.; Fitzgerald G. *Chem. Phys. Lett.*, 1993, 208, 359.

[33] Weigend F.; Hasser M.; Patzelt H.; Ahlrichs R. *Chem. Phys. Lett.*, 1998, 294, 143.

[34] Boys S. F.; Bernardi F. *Mol. Phys.*, 1970, 19, 553.

[35] Jurecka P.; Hobza P. *Chem. Phys. Lett.*, 2002, 365, 89.

[36] Lee E. C.; Kim D.; Jurecka P.; Tarakeshwar P.; Hobza P.; Kim K. S. *J. Phys. Chem. A*, 2007, 111, 3446.

[37] Hesselmann A.; Jansen G. *Chem. Phys. Lett.*, 2002, 357, 464; 2002, 362, 319; 2003, 367, 778.

[38] Hesselmann A.; Jansen G.; Schutz M. *J. Chem. Phys.*, 2005, 122, 014103.

[39] MOLPRO a package of ab initio programs designed by Werner H. J., Knowles P. J. version 2006.1; Amos R. D.; Bernhardsson A.; Berning A.; Celani P.; Cooper D. L.; Deegan M. J. O.; Dobbyn A. J.; Eckert F.; Hampel C.; Hetzer G.; Knowles P. J.; Korona T.; Lindh R.; Lloyd A. W.; McNicholas S. J.; Manby F. R.; Meyer W.; Mura M. E.; Nicklass A.; Palmieri P.; Pitzer R.; Rauhut G.; Schutz M.; Schumann U.; Stoll H.; Stone A. J.; Tarroni R.; Thorsteinsson T., and Werner H.-J.

[40] a national scientific user facility sponsored by the Department of Energy's Office of Biological "A portion of the research was performed using EMSL, Environmental Research, and located at Pacific Northwest National Laboratory.". *Chinook supercomputer.*

[41] Sedlak R.; Jurecka P.; Hobza P. *J. Chem. Phys.*, 2007, 127, 075104.

[42] It is difficult to precisely comment on the temperature during the expansion process but it should lie between the nozzle temperature (298 K) and the terminal temperature (3.5 K for phenylacetylene).

[43] Schutz M. Hesselmann A., Jansen G. *J. Am. Chem. Soc.*, 2006, 128, 11730.

Appendices